AIAA JOURNAL
Vol. 37, No. 8, August 1999

Evaluation of Strain Energy Release Rates in Delaminated Laminates Under Compression

Mark J. Johnson* and Srinivasan Sridharan†
Washington University, St. Louis, Missouri 63130

Various approaches to the determination of the energy release rates of compressively loaded composite laminates are critically reviewed. These are the J integral, crack-closure integrals, and the direct method, which involves integration of the load-end compression relationship. The J integral is found to be a reliable approximation for the total energy release rate. The use of the crack tip stress field for the determination of modal contributions is explored for cracks between plies of same and differing material properties, respectively. The assumptions on which this technique is based are critically examined. Finally, a new displacement based method for the computation of modal contributions to G is proposed. This approach is found to be very reliable and provides values of G_I and G_{II} with a relatively coarse mesh. This new technique is expected to supplant the currently used stress-based mode separation technique.

Introduction

In a laminated composite there are three principal failure modes: intra-ply (transverse matrix) cracking, interlaminar matrix delamination (fiber-matrix debonding), and fiber failure (including kink band and microbuckling). Of these, interlaminar matrix delamination is of major importance,[1] as it is a most prevalent damage growth mode.[2]

Resistance to delamination growth is measured by the strain energy release rate, which is the energy dissipated per unit area of delamination growth. When the energy release rate is greater than the fracture toughness of the material, delamination growth will occur. If the energy release rate remains greater than the fracture toughness as the delamination grows, for constant loading, then unstable growth occurs. Conversely, if the energy release rate falls below the value of the fracture toughness, for constant loading, delamination growth ceases. Delamination growth will then not occur unless the load is increased.

A review of the literature indicates that there are three approaches to the determination of strain energy release rate. These are 1) path-independent J integral,[3] 2) crack-closure integrals that provide total G, as well as the modal contributions G_I and G_{II},[4] and 3) direct calculation of G by integration of the load-displacement relation, using two models containing crack lengths of a and $a + \Delta a$, respectively.

The J integral is found to be a plausible alternative measure of the total energy release rate. However, it does not give details on mode I and mode II contributions to the total energy release rate.[5] Crack-closure integrals utilize crack tip stresses, as integration is performed over a length that must tend to zero in the limit, and the determination of these stresses requires a very fine mesh. Furthermore, Sun[6] has shown that for a bimaterial crack the stress variation in the immediate vicinity of the crack tip is oscillatory in nature, and the values of G_I and G_{II} as obtained by the crack-closure integrals (as given in Ref. 4) do not converge as the crack extension Δa tends to zero. This raises the question of the rationality and usefulness of G_I and G_{II} from the standpoint of computation and prediction of crack growth. Finally, the direct calculation of G is simple to implement but does not provide the modal contributions on which the crack growth criteria are based.

It is found that computations of stress-based crack-closure integrals, to determine mode I and mode II energy release rates, require an order of magnitude greater computational effort than would be required to both describe the overall structural behavior and compute the energy release rate by the direct method. This leads to the question of whether it would be possible to decompose the displacement-based G into G_I and G_{II}. This paper describes a numerical case study in which these questions are explored in depth.

Case Study

Geometry

A compressively loaded plate subject to plane strain conditions and containing one asymmetric through-width delamination was studied. Because of symmetry conditions, only one half of the plate was modeled. The model represents a plate of dimensions 1×1 m, with a thickness of 0.03 m, and contained a central delamination of depth 0.005 m, whose initial total length was 0.3 m (Fig. 1).

Material

Figure 1 shows the axes of coordinates, x and z axes, running along the longitudinal and transverse directions, respectively (y axis is normal to the paper). The plate is composed of laminae with fiber orientations of 0 and 90 deg, defined with respect to the x direction. Unless otherwise noted, all laminae have fiber orientation of 0 deg. The laminae are assumed to be transversely isotropic with respect to fiber axis. The material considered is Kevlar®/epoxy ($E_1 = 70.0$, $E_2 = 4.5$, $G_{12} = 2.5$ GN/m^2; $\nu_{12} = 0.35$, $\nu_{23} = 0.50$).

Analysis

The problem was studied using an hp-version finite element model developed by the authors, (which employed higher order polynomial shape functions starting with cubics), and ABAQUS (Version 5.6-1, licensed from Hibbitt, Karlsson, and Sorenson, Inc.), a general purpose commercial package. The parent hp-version model consisted of four elements obtained by the intersection of the line of the crack and a line running parallel to the z axis at the crack tip. The four elements thus obtained were further subdivided to obtain models of 16 and 64 elements. The displacement functions are in the form of Lagrange interpolation polynomials of degree $p = 3$ and above. With $p = 3$ the degrees of freedom numbered 98, 338, and 1226, respectively for the 4, 16, and 64 element models. The elements used in all ABAQUS models were eight-node biquadratic plane strain quadrilaterals. These models included totals of 240, 3000, and 4110 elements, and 808, 9364, and 12,792 nodes (corresponding degrees of freedom: 1700, 19,048, and 25,952).

Strain-Displacement Relations

Geometrically nonlinear analyses were performed in all cases to trace the delamination buckling growth by incorporating minute imperfections. Two sets of strain-displacement relations were considered in the hp version. The first approximation involves only a

Received 16 April 1998; revision received 5 January 1999; accepted for publication 5 February 1999.

*Research Fellow; currently Project Engineer, Boeing Company, Phantom Works, St. Louis, MO 63166-0516. Member AIAA.
†Professor of Civil Engineering. Member AIAA.

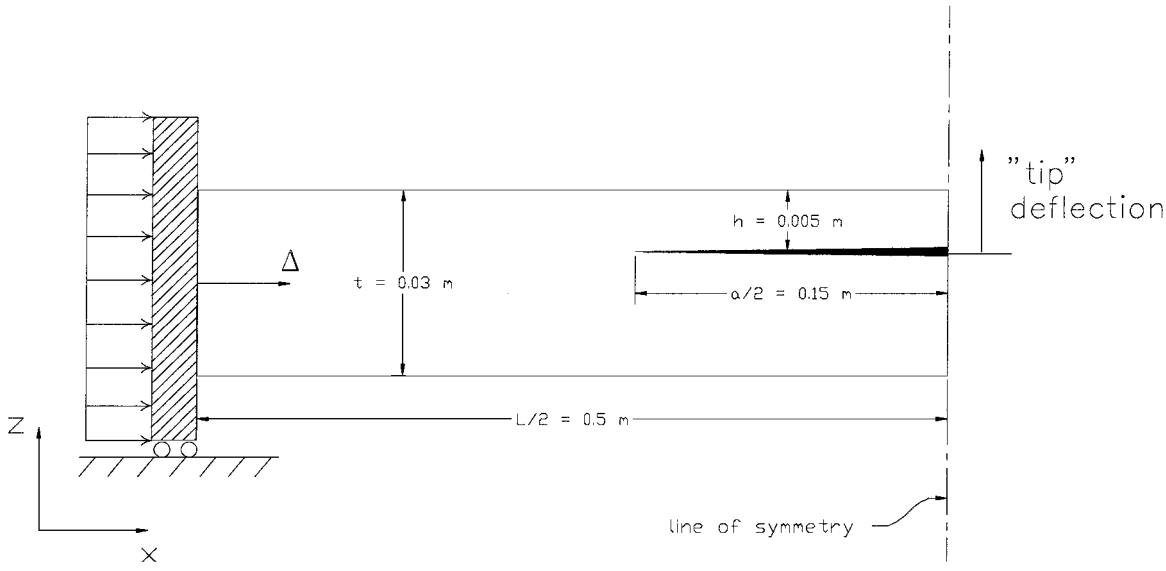

Fig. 1 Single delamination model (model 1).

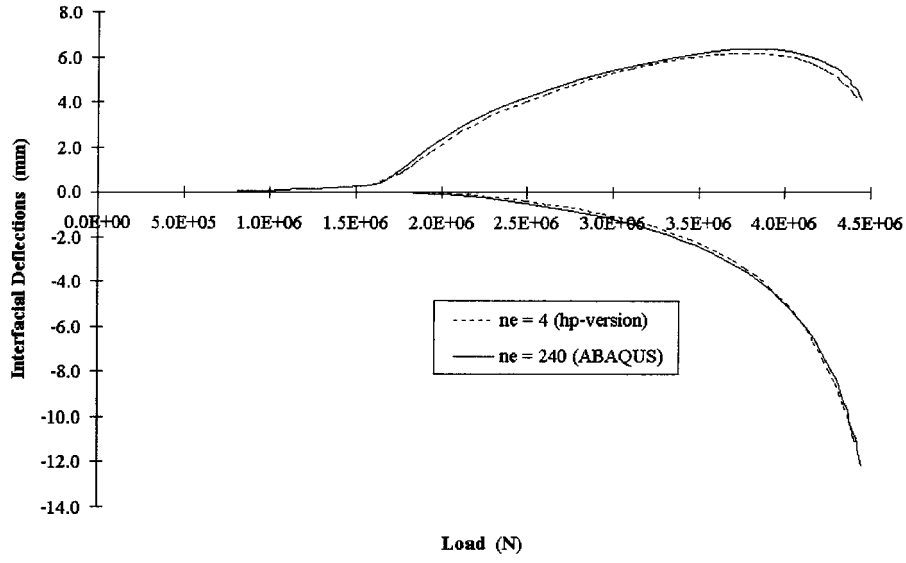

Fig. 2 Tip deflection vs load.

portion of the nonlinear terms. These first approximation strain-displacement relations are given in Eqs. (1–3):

$$\epsilon_x = \frac{\partial u}{\partial x} + \frac{1}{2}\left(\frac{\partial w}{\partial x}\right)^2 \tag{1}$$

$$\epsilon_z = \frac{\partial w}{\partial z} \tag{2}$$

$$\gamma_{xz} = \frac{\partial u}{\partial z} + \frac{\partial w}{\partial x} \tag{3}$$

The second approximation included the complete set of nonlinear terms:

$$\epsilon_x = \frac{\partial u}{\partial x} + \frac{1}{2}\left[\left(\frac{\partial w}{\partial x}\right)^2 + \left(\frac{\partial u}{\partial x}\right)^2\right] \tag{4}$$

$$\epsilon_z = \frac{\partial w}{\partial z} + \frac{1}{2}\left[\left(\frac{\partial u}{\partial z}\right)^2 + \left(\frac{\partial w}{\partial z}\right)^2\right] \tag{5}$$

$$\gamma_{xz} = \frac{\partial u}{\partial z} + \frac{\partial w}{\partial x} + \left(\frac{\partial u}{\partial x}\frac{\partial u}{\partial z} + \frac{\partial w}{\partial x}\frac{\partial w}{\partial z}\right) \tag{6}$$

ABAQUS incorporates the full set of nonlinear terms in all cases.

Structural Response

The structural response is typified by the load-end displacement and load tip deflection relations. Here the tip deflections refer to the upper and lower crack surface deflections at the plane of symmetry (Fig. 1). Convergence of these deflections was studied for both the hp version and ABAQUS models. Figures 2 and 3 compare the results for two levels of discretization: four element hp-version and 240 element ABAQUS model, respectively (ne = number of elements). These results are in close agreement and illustrate the superiority of the higher order elements. A linear stability analysis was also performed to determine the delamination buckling and overall buckling loads; these were found to be 1.7 *MN* and 5.7 *MN*, respectively.[7] As can be seen, the deflections of the thin top sublaminate increase rapidly in the vicinity of the delamination buckling load (Fig. 4), and the entire plate develops large deflections as the overall buckling load is approached (Fig. 5).

Energy Release Rate

The energy release rate is the driving force for delamination fracture. A measure of the energy release rate thus provides information on the tendency of a delamination to grow. Computed as a function of crack length, it can also be used to determine the stability of delamination growth under constant loading conditions. In this section the various approaches to the determination of the energy release rates are critically reviewed.

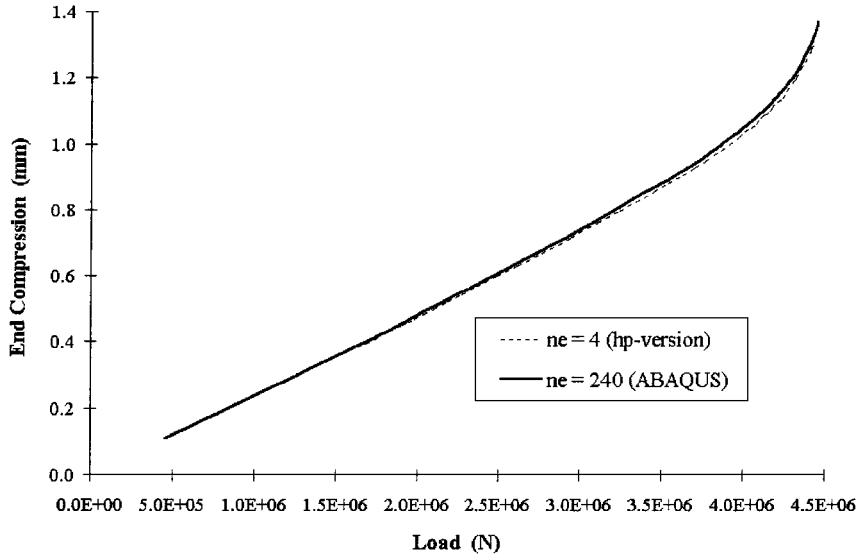

Fig. 3 End compression vs load.

Fig. 4 Delamination buckling mode.

Fig. 5 Global buckling deformation.

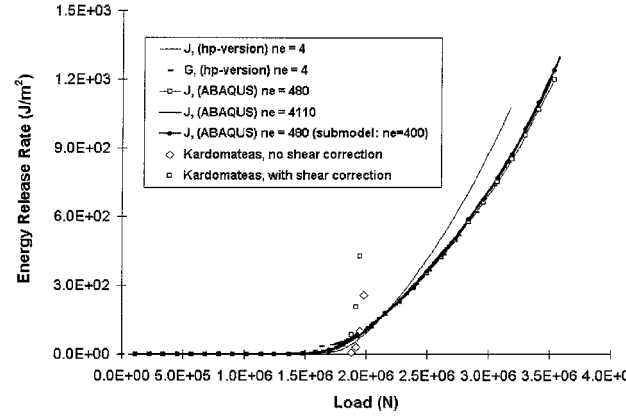

Fig. 6 J integral/direct *G*.

J Integral

The J contour integral has been used with some success to characterize fracture in nonlinear materials.[8,9] It is both an energy parameter and a stress intensity parameter. Rice[3] idealized elastic-plastic deformation as nonlinear elastic, forming the basis for the extension of fracture mechanics concepts well beyond the limits of linear elastic fracture mechanics. Elasto-plastic response may be treated as nonlinearly elastic, as long as unloading at the crack faces may be neglected.

Considering an arbitrary counterclockwise path Γ around the tip of a crack with the x and y axes given and the crack extending in the $-x$ direction, the J integral is defined as[3]

$$J = \int_{\Gamma} \left(W \, \mathrm{d}y - T_i \frac{\partial u_i}{\partial x} \, \mathrm{d}s \right) \tag{7}$$

where W is the strain energy density, u_i are the displacement vector components, ds is an incremental length along the contour Γ, and T_i are components of the pseudotraction vector, given by

$$T_i = \sigma_{ij} n_j \tag{8}$$

Here σ_{ij} are the components of the first Piola–Kirchhoff stress and n_j are the components of the normal vector to Γ (both defined on the undeformed configuration). The strain energy density may be taken in the form

$$W = \int_0^{\epsilon_{ij}} \sigma_{ij} \, \mathrm{d}\epsilon_{ij} \tag{9}$$

where σ represents the second Piola–Kirchhoff stresses and ϵ the Green–Lagrange strains.

To examine the validity of the J integral as a measure of strain energy release rate, the J integral approach, as outlined in Ref. 10, is used to compute the total strain energy release rate for the hp-version model. The variation of the J integral with load (for the case study shown in Fig. 1) is considered in Fig. 6 (designated J, hp-version). Appropriate initial imperfections were introduced to facilitate the transition from the unbuckled to the buckled configuration. Figure 6 shows that the J integral, as computed by the hp-version method and the ABAQUS contour integral, agrees well with the total energy release rate computed using the direct method of calculation (the standard for determining the accuracy of the total energy release rate), which will be discussed in detail in the following sections.

J integral results based on a beam/plate approach[9] are also shown in Fig. 6 for reference. Although this method accurately predicts total energy release rate near delamination buckling (which admittedly may be the critical loading region of interest), the results otherwise appear to differ greatly from the more reliable method of direct calculation. Though simpler models have been utilized with some success,[11–13] we are unable to confirm the results at this time.

The virtual crack extension method has also been applied[14–17] to similarly determine the energy release rate for linear elastic, nonlinear elastic, and elastic-plastic materials.

Direct Calculation

As detailed, the direct calculation of the total strain energy release rate is much more reliable than those methods dependent on the accurate representation of the crack tip stress singularity. The total strain energy release rate is simply the measure of the energy released for a crack extension of Δa. This is given as

$$G = -\frac{\partial \Pi}{\partial a} \tag{10}$$

For the finite element models employed in this work, the total potential energy Π of a structure was found directly by the integration of the load-deflection (end compression) diagram, as in Eq. (11).

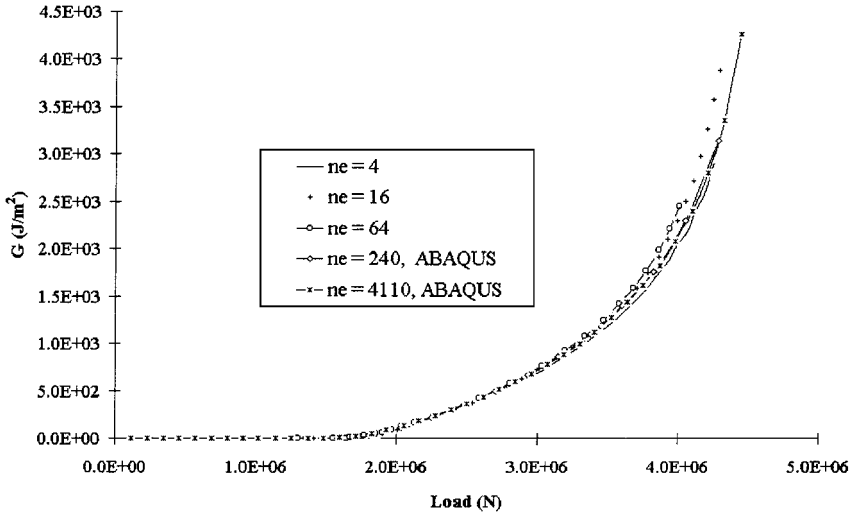

Fig. 7 Direct G, hp version and ABAQUS.

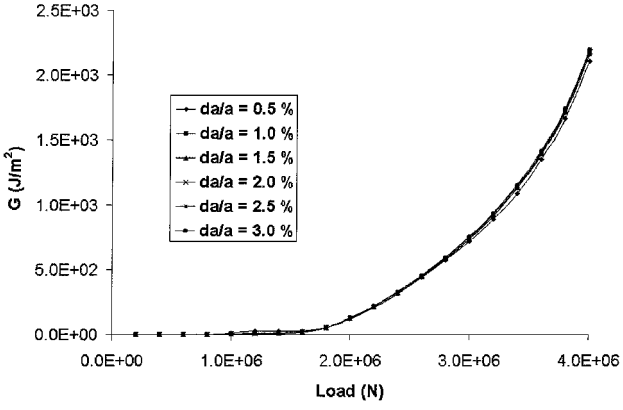

Fig. 8 Convergence of direct G.

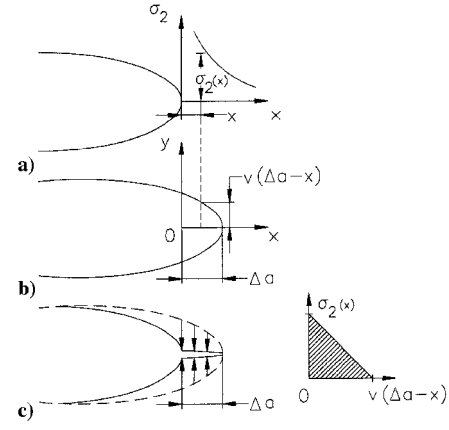

Fig. 9 Crack-closure method.

Note that P represents the applied load, Δ the end compression, and $d\Delta$ an increment of end compression:

$$\Pi = \int_0^{\Delta} P \, d\Delta - P\Delta \tag{11}$$

Two companion models are considered with crack lengths a and $a + \Delta a$, respectively. The potential energies Π_1 and Π_2 of the two models are computed, and the energy release is obtained as

$$G = -\frac{\Pi_2 - \Pi_1}{\Delta a} \tag{12}$$

Results of this method, using ABAQUS and the hp-version, are compared in Fig. 7. The results are rapidly convergent, with the coarsest model, consisting of only four elements, producing results of acceptable accuracy for practical applications. Even though the desire is for Δa to be very small, for practical computations it is reasonable to set $\Delta a/a$ between 1 to 2%. Convergence of the direct method of calculation is considered in Fig. 8; rapid convergence, from $\Delta a/a = 0.5$ to 3.0%, is evident. The direct method, then, is the most reliable and robust; the value of the total energy release rate obtained may be viewed as a benchmark value for testing the accuracy of other approaches.

Modified Crack-Closure Method: General

Irwin postulated that the energy release rate associated with a crack extension of Δa was equal to the amount of energy required to close the crack by an amount Δa. Using a polar coordinate system with the origin at the extended crack tip, this results in the equation[4]

$$G = \lim_{\Delta a \to 0} \frac{1}{2\Delta a} \int_0^{\Delta a} \sigma_y(\Delta a - r, 0)\bar{v}(r, \pi) \, dr + \lim_{\Delta a \to 0} \frac{1}{2\Delta a} \int_0^{\Delta a} \tau_{xy}(\Delta a - r, 0)\bar{u}(r, \pi) \, dr \tag{13}$$

where G is the energy release rate, σ_y and τ_{xy} are the stresses near the crack tip, $\bar{u}$ and $\bar{v}$ are the relative sliding and opening displacements between adjacent points on the crack faces, and Δa is the crack extension. The first term is equivalent to G_I, whereas the second term is equivalent to G_{II}.

In Fig. 9a the first model of crack length a is shown, along with the second model of crack length $a + \Delta a$, Fig. 9b. For mode I energy release rate σ_2 is found in the first model, and the corresponding displacement in the vertical direction is found in the second model; G_I is thus evaluated. Mode II energy release rate is determined in a similar fashion. Equation (13) assumes a linear relation between stress and displacement, as shown in Fig. 9c for mode I. Thus, the factor of $\frac{1}{2}$ is introduced in the equations. Using this method, it is also sufficient to treat only one model, obtaining the stress variation ahead of the crack and the displacement variation downstream of the crack for use in Eq. (13) (which simply implies that self-similar crack growth is assumed).

This approach depends on the accurate modeling of the structural behavior near the crack tip. If conventional (nonsingular) elements are used to model the crack tip, the integrated stress distribution obtained at the crack tip may not accurately reflect this singularity. The use of singular elements may provide a better estimate of this singularity. However, the nature of this singularity in geometrically nonlinear problems remains unknown. The actual stress distribution near the crack tip may be captured by the use of nonsingular elements and a very fine mesh. Davidson,[18,19] Davidson and Krafchak,[12] and Davidson et al.[13,20] have shown some interesting results employing a crack tip element in the study of various delamination problems. However, the authors are hesitant to follow this approach, in part because it involves the artificial adjustment of material properties (in particular ν_{13}) to obtain convergent finite element models.

The crack-closure method was employed using eight-node plane strain quadrilateral elements in ABAQUS. The actual stresses were

extrapolated along the crack tip from the Cauchy stresses computed at the appropriate Gaussian points. The products of the stresses and the corresponding displacements (both functions of x) were integrated over Δa; the result was then divided by Δa.

The reliance of this method on calculated stress values in the immediate vicinity of the crack tip calls into question its accuracy. At best, this method may be an acceptable approximation for the determination of the energy release rates, the valuable contributions made by many researchers[21–23] in this area notwithstanding. To avoid the use of these crack tip stresses, Hashemi[24] and Kinloch[25] suggested partitioning G on a global energy basis, as opposed to using the local stress field solutions.

Sun[6] has shown that the values of G_I and G_{II} do not in fact converge in the form of such crack-closure integrals for a crack lying along the interface of two elastic bodies with different elastic properties. However, he does show that the total strain energy release rate G is well defined for this problem.

Others have also provided insight with regard to bimaterial delaminations. In the case of a one-dimensional delamination model, Yin[5] determined the total energy release rate by evaluating the J integral of the postbuckling solution based on lamination theory without knowledge of the nature or asymptotic form of the interlaminate stress between two dissimilar layers separated by a delamination. Suo and Hutchinson[11] solved the problem of a semi-infinite interface crack between two infinite isotropic (yet dissimilar) elastic layers under general edge loading analytically (except for a single real scalar independent of loading, which was extracted from a numerical solution). Considering mixed mode failure along a bimaterial interface, Charalambides et al.[26] found that a global method of analysis based upon consideration of the applied energy release rates produced results more consistent with experimental data than a method that utilized the local singular stress field ahead of the crack tip.

Crack-Closure Method: Numerical Experience

Variations in the stresses in the immediate vicinity of the crack tip are seen to exist across the spectrum of models and methods considered in this work. Given this sensitivity, some criteria are needed before any computed values of G_I and G_{II} may be deemed reliable. We propose that 1) G_I and G_{II} must converge separately and 2) $G_I + G_{II}$, obtained from stress-based mode separation, must equal G, as found by the displacement based (direct) method.

Discretization Effects: Illustrations

In this section we examine the effect of mesh refinement on the mode separation results. It is first necessary to establish the validity of the mode separation results, compared to the direct calculation of the energy release rate. Because it is known that the higher level of discretization will be necessary for mode separation, this comparison is made for the ABAQUS model containing 4110 elements. In Fig. 10 the comparison is made between the mode separation results using two models ($G_I + G_{II}$) and the direct calculcation G.

Figure 10 shows that this degree of mesh refinement captures the total energy release rate ($G_I + G_{II}$) with sufficient accuracy, as it is close to that of the method of direct calculation, even well beyond the range of loading of interest. The actual stress distribution is best captured by nonsingular elements and a very fine mesh.

The hp-version finite element method developed for this work contained varying mesh refinements, including 4, 16, and 64 element models. Stress-based mode separation using these models proved difficult. The stress-based mode separation results of the 4 and 16 element models were meaningless. The results utilizing the 64 element model were not significantly better (Fig. 11). Evidently, the mesh refinement required to obtain values of G_I and G_{II} satisfying the aforementioned criteria is of an order of magnitude higher than that required for an accurate description of the structural response. A mesh refinement of at least 3000 elements was necessary to get convergent and consistent values of G_I and G_{II}.

In Fig. 12 the convergence of the total energy release rate, as obtained by the stress-based method, is considered for varying $\Delta a/a$.

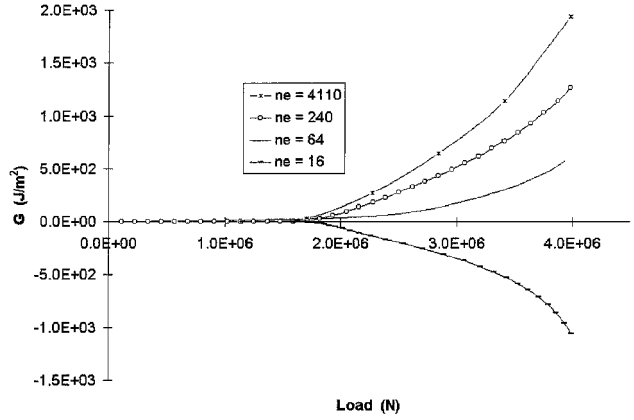

Fig. 11 Discretization comparison: $G_{I,\sigma} + G_{II,\sigma}$.

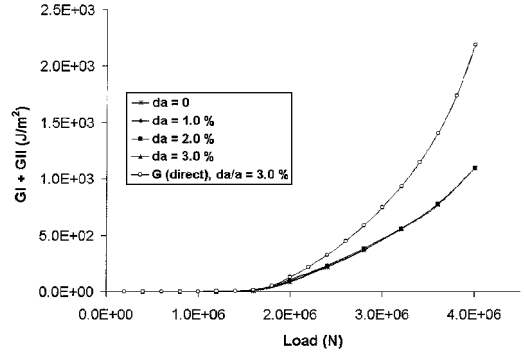

Fig. 12 Convergence of stress-based G: $G_{I,\sigma} + G_{II,\sigma}$.

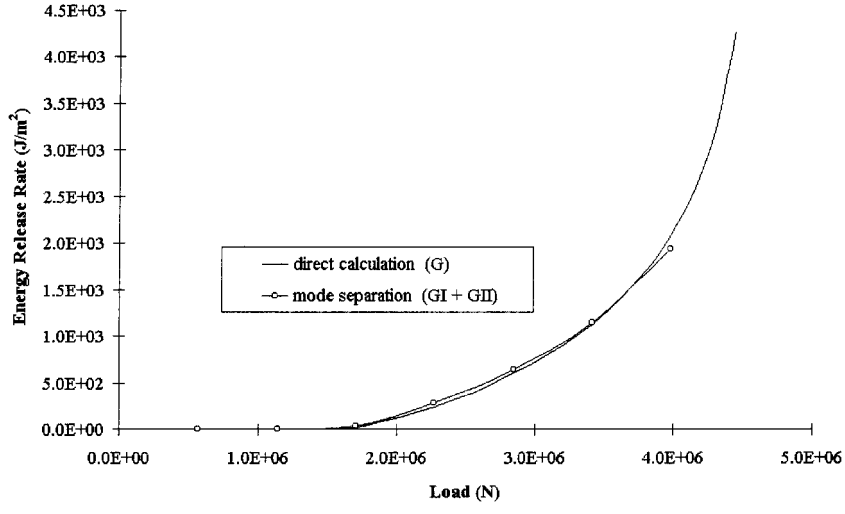

Fig. 10 Total energy release rate comparison: G_Δ and $G_{I,\sigma} + G_{II,\sigma}$.

Again, rapid convergence is evident. However, for this 480-element model the stress-based method converges to an incorrect value, as compared to the displacement-based approach, as shown.

We next investigate issues associated with the use of the crack-closure method (stress-based method of mode separation).

Linearity of the Stress-Displacement Relation

One of the assumptions involved is that of a linear relation between stress and displacement, as in Eq. (13). The accuracy of this assumption was investigated in detail, as the present problem is clearly nonlinear. The stress-displacement relations did indeed follow a sensibly (stepwise) linear relation throughout the range of loading. Thus the conclusion was made that the inaccuracies produced by the use of the crack-closure integrals were caused by the inaccurate representation of the crack tip stresses and the inherent mesh dependency of these stresses.

Bimaterial Crack

One of the bimaterial laminates considered was a crossply laminate containing six layers of kevlar/epoxy laminae [0//90/0/0/90/0] (where // signifies the location of the delamination), with dimensions as in Fig. 1. The delamination was located between layers 1 and 2 (across the 0/90 interface). These thick laminae served to accentuate the bimateriality of the laminate. The total energy release rate obtained via stress-based mode separation (for three levels of discretization) is compared to that of the direct calculation in Fig. 13.

The values of G_I and G_{II} are found to converge separately[7] (not shown), and the values obtained for the 3000 and 4110 element models, respectively, were shown to be in agreement with an error of less than about 1% However, the corresponding values $G_I + G_{II}$ are higher than the total G, as obtained by the direct method, by about 20% for loads just beyond the critical load. This points to the basic underlying problem associated with mode separation for bimaterial cracks.

As the thicknesses of the plies were made smaller, however, this difference diminished. As the number of plies increased, G_I and G_{II} could be predicted with the material appropriately homogenized[7] with the predictions satisfying our criteria 1) and 2). These results indicate that G_I and G_{II} may be more well behaved in the context of engineering computation than presaged by the work of Sun.[6] Further, in a majority of practical cases, the laminate is composed of numerous layers, and for such cases G_I and G_{II} can be determined uniquely and thus do appear to have practical significance.

Displacement-Based Mode Separation: A New Approach

The inherent difficulties associated with the evaluation of the crack-closure integrals are well known. However, no alternative method of mode separation is currently available in the literature. If a new approach were to be formulated, it would need to avoid the difficulties encountered in the use of the crack-closure integrals. This section presents such a new method.

It is possible to compute the mode I energy release rate directly by suppressing the mode II contribution and vice versa by an appropriate conditioning of the crack tip. We consider two models with half-crack lengths of $a/2$ and $(a + \Delta a)/2$, as before. To ensure that the derivative $\partial \Pi / \partial a$ exists across the crack tip, we need to ensure that the crack extends with the crack tip conditions unaltered. A step-by-step procedure for the determination of G_I and G_{II} is outlined next.

Analysis of Model 1

Figure 14 shows model 1, which represents one-half of a delaminated plate with half-crack length of $a/2$. (Figure 14 presents only selected elements near the crack tip.) The nonlinear analysis of the model under prescribed load P is performed as before, but with one vital difference. To determine G_I, we now impose the condition that the relative displacement u between the pairs of nodes on opposite faces of the crack be set to zero over a small length of $\Delta a/2$, measured from the crack tip. The potential energy (Π_1) of this structure is then computed for varying values of P.

Analysis of Model 2

We now consider a model with the crack tip extended by an amount $\Delta a/2$ (see model 2 in Fig. 14). Nonlinear analysis is once again performed, but now the restraint $\Delta u = 0$ is imposed over a length Δa, starting from the crack tip. The potential energy (Π_2) of this structure is then computed for the same values of P as for model 1.

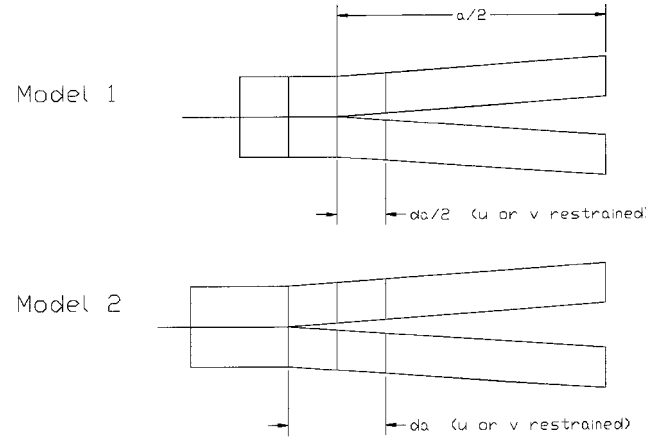

Fig. 14 Restrained models 1 and 2.

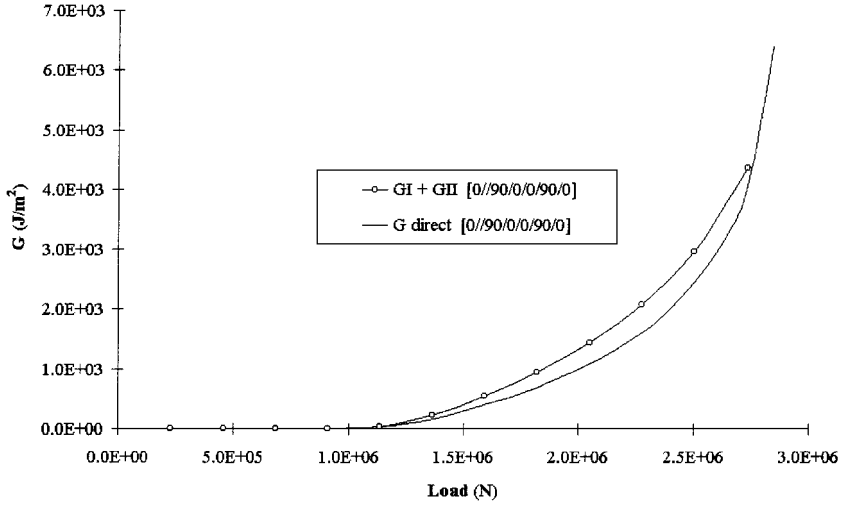

Fig. 13 Bimaterial crack: G_Δ and $G_{I,\sigma} + G_{II,\sigma}$.

Determination of G_I and G_{II}

The strain energy release rate in this case is equal to G_I, which is given as

$$G_{I,\Delta} = -\frac{\Delta\Pi}{\Delta a}\bigg|_{\Delta u=0} = -\frac{\Pi_2 - \Pi_1}{\Delta a}\bigg|_{\Delta u=0} \tag{14}$$

To determine G_{II}, the procedure is repeated with the restraint $\Delta v = 0$. The energy release rates thus obtained are denoted as $G_{I,\Delta}$ and $G_{II,\Delta}$. These are distinguished from the stress-based mode separation values, designated as $G_{I,\sigma}$ and $G_{II,\sigma}$:

$$G_{II,\Delta} = -\frac{\Delta\Pi}{\Delta a}\bigg|_{\Delta v=0} = -\frac{\Pi_2 - \Pi_1}{\Delta a}\bigg|_{\Delta v=0} \tag{15}$$

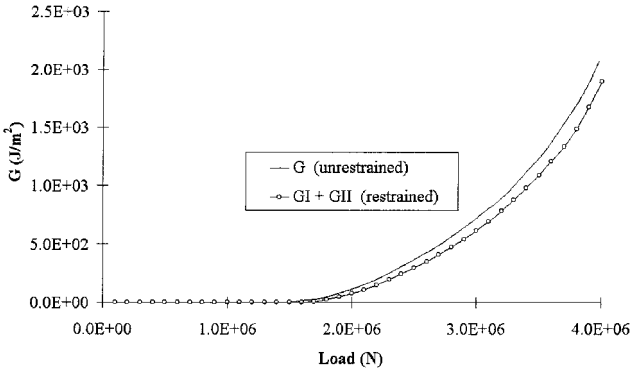

Fig. 15 $(G_{I,\Delta} + G_{II,\Delta})$ and G.

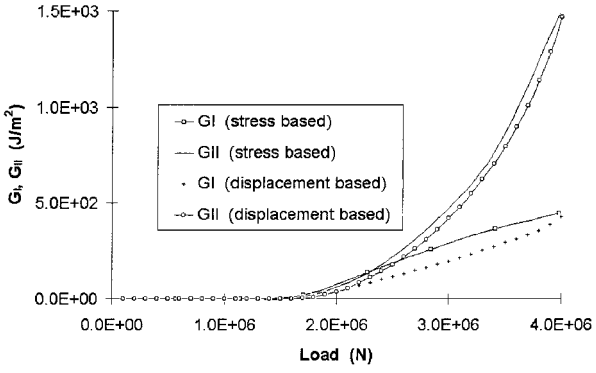

Fig. 16 Displacement- and stress-based G_I, G_{II}.

Verification

The displacement-based mode separation technique may be verified against the displacement-based, or direct, method of calculation of the total energy release rate. To accomplish this, the mode I and II contributions obtained via the displacement-based method are summed and compared to the total energy release rate found by direct calculation. As an example, we consider once again the kevlar/epoxy $[0]_{30}$ laminate (ABAQUS) model consisting of 4110 elements. The total G as obtained in this fashion $(G = G_{I,\Delta} + G_{II,\Delta})$ is compared to the total energy release rate found by the direct method in Fig. 15. This new method of mode separation reasonably calculates the total energy release rate for this level of discretization.

Figure 16 compares the mode I and mode II contributions obtained by this method to those found by the stress-based method of mode separation (which has been shown to be highly sensitive to the computation of the crack tip stress field). In the immediate vicinity of delamination buckling, there are some noticeable differences in the results of the two approaches. For both G_I and G_{II} the displacement-based approach produces values less than that of the stress-based approach. This is reasonable because the displacement-based approach imposes restraints that are never cancelled.

It is easy to infer that the displacement-based mode separation is much more robust and reliable compared to the stress-based method of mode separation. The real test of this method is whether or not a lesser refined mesh can produce similar results using the same approach. The stress-based method is only accurate with a very fine mesh refinement (as it relies on the accurate modeling of the stresses near the crack tip). If the displacement-based method can produce good results with a significant reduction in computational cost, then clearly this new method has great potential. This method does not rely on the accurate representation of the integrated stresses near the crack tip; it relies on an accurate estimate of the overall behavior of the structure, and thus it should be possible to significantly reduce the computational effort in assessing the modal contributions to the energy release rate.

To this end, a much coarser 480-element model was created to study the problem. The mesh near the crack tip was as fine as was required to impose the necessary constraints on the displacements in order to isolate G_I and G_{II}. This model contained approximately $\frac{1}{8}$ the number of degrees of freedom of the 4110-element model, representing a significant reduction in mesh refinement, as well as computational cost. Using the displacement-based method, the values of G_I and G_{II} were recovered without noticeable loss of accuracy. Further, $G_{I,\Delta}$ and $G_{II,\Delta}$ were found to converge separately (not shown). The displacement-based method was also found to produce excellent results for the total energy release rate $(G_{I,\Delta} + G_{II,\Delta})$ with a much less refined mesh (Fig. 17). Again, the 480 element model contained $\frac{1}{8}$ the number of degrees of freedom and took approximately $\frac{1}{10}$ of the CPU time of the 4110-element model. The method is clearly robust and does not require the fine mesh and high level of

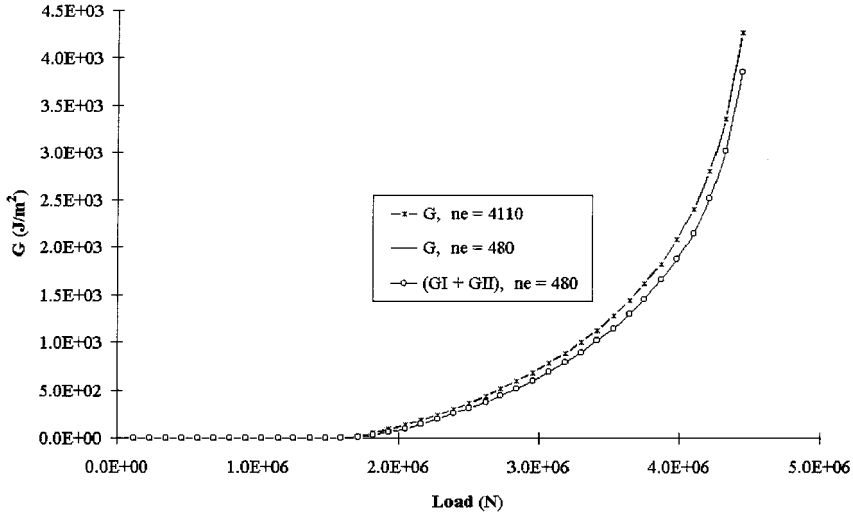

Fig. 17 Displacement-based $(G_{I,\Delta} + G_{II,\Delta})$: homogeneous.

computational effort required by the stress-based method of mode separation.

Bimaterial Crack

This method was also verified for a bimaterial crack, again considering the crossply laminate containing six layers of Kevlar/epoxy laminae [0//90/0/0/90/0] with dimensions as in Fig. 1. The stress-based method again produced slightly higher results for G_I and G_{II}, and the greatest discrepancy was in G_I.

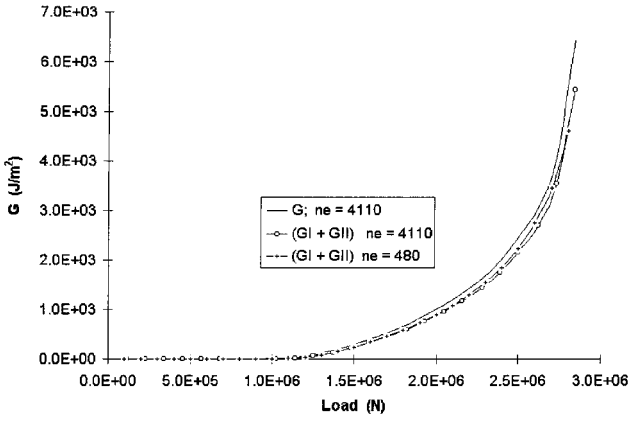

Fig. 18 Displacement-based ($G_{I,\Delta} + G_{II,\Delta}$): bimaterial.

Once again the modal contributions $G_{I,\Delta}$ and $G_{II,\Delta}$ were summed and compared to G obtained by the direct method. Two levels of discretization were employed as before, these consisting of 4110 and 480 elements. Note that these results (Fig. 18) are in close agreement, indicating convergence. Again the sum $(G_{I,\Delta} + G_{II,\Delta})$ is close to but slightly lower than the unrestrained displacement-based G, whereas the stress-based $(G_{I,\sigma} + G_{II,\sigma})$ was higher. For computation of mode I and mode II energy release rates, the displacement-based method is more reliable than the stress-based approach.

It appears that a conservative prediction can always be obtained if G and G_{II} are evaluated by the displacement-based approach, and G_I is found as $G_I = G - G_{II}$. This result will produce a slightly exaggerated value of G_I, and because G_I governs the crack growth predictions, the prediction will be somewhat conservative.

A related application of the new method involved the imposition of the appropriate displacement restraints to provide the modal contributions, as computed utilizing the J integral (in effect, J_I and J_{II}). The J integral is utilized in this fashion to obtain mode I and mode II energy release rates, as well as the summed total. These results are portrayed in Figs. 19–24 for the homogeneous and bimaterial [0//90/0/0/90/0] laminates, as obtained from the 480-element model. $J_{I,\Delta}$ and $G_{I,\Delta}$ are seen to be nearly coincident, as are $J_{II,\Delta}$ and $G_{II,\Delta}$ (and thus the respective summed total energy release rate) for the homogeneous laminate. For the bimaterial laminate $J_{I,\Delta}$ and $G_{I,\Delta}$ differ slightly as the overall buckling load is approached, whereas $J_{II,\Delta}$ and $G_{II,\Delta}$ are coincident. These results lend credence to the displacement-based method and offer an alternative approach to its application, in that the path-independent

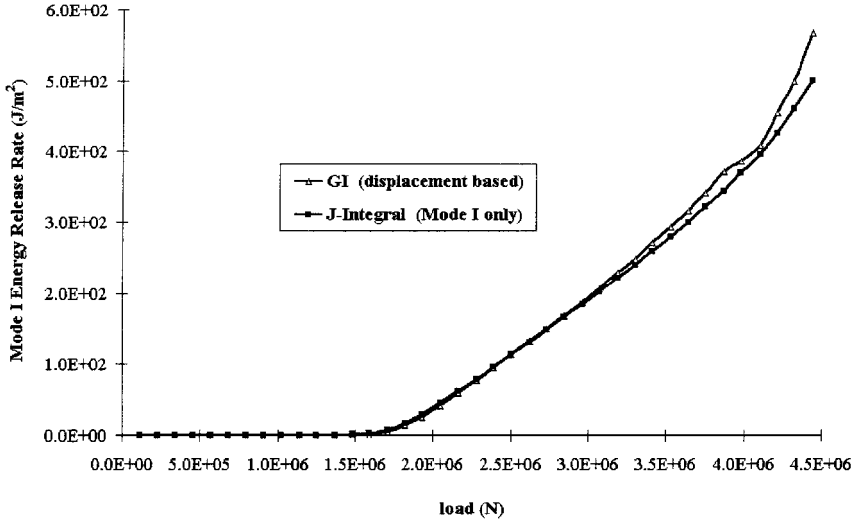

Fig. 19 Displacement-based $J_{I,\Delta}$: homogeneous.

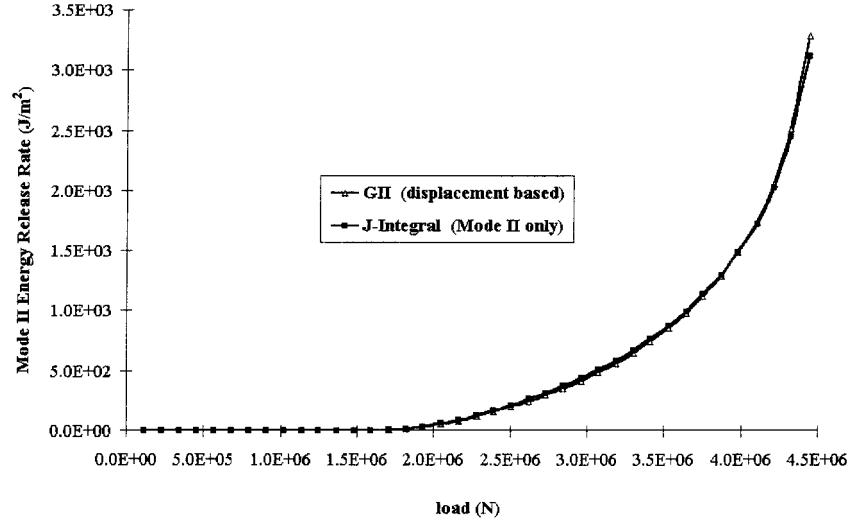

Fig. 20 Displacement-based $J_{II,\Delta}$: homogeneous.

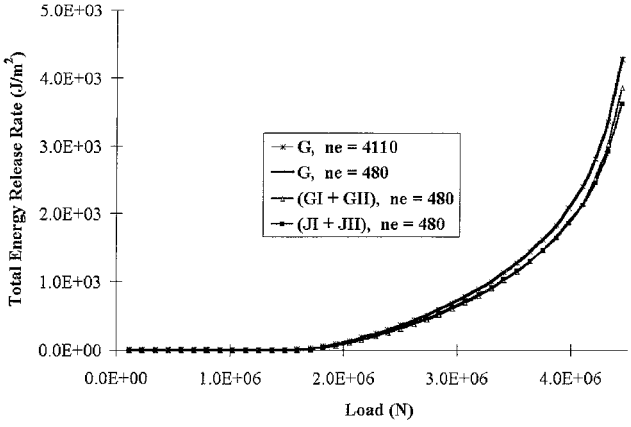

Fig. 21 Displacement-based ($J_{I,\Delta} + J_{II,\Delta}$): homogeneous.

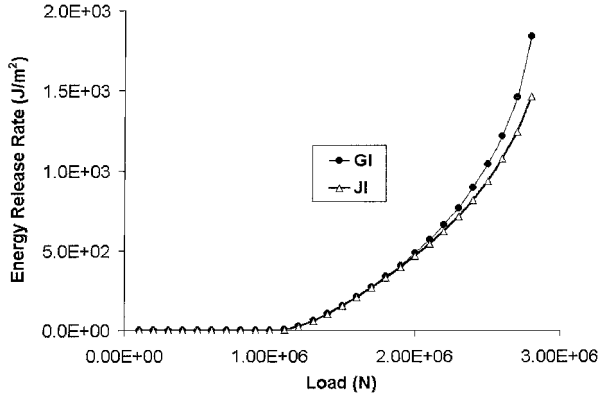

Fig. 22 Displacement-based $J_{I,\Delta}$: bimaterial.

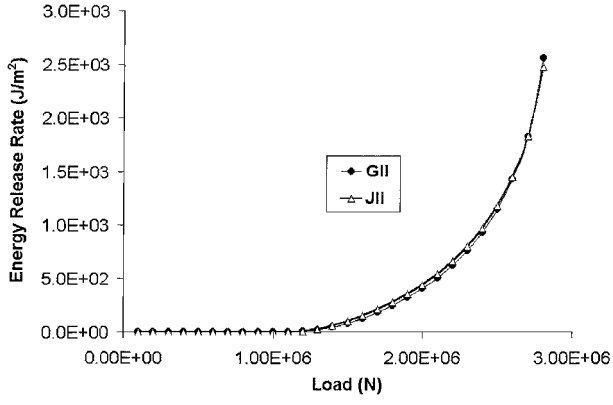

Fig. 23 Displacement-based $J_{II,\Delta}$: bimaterial.

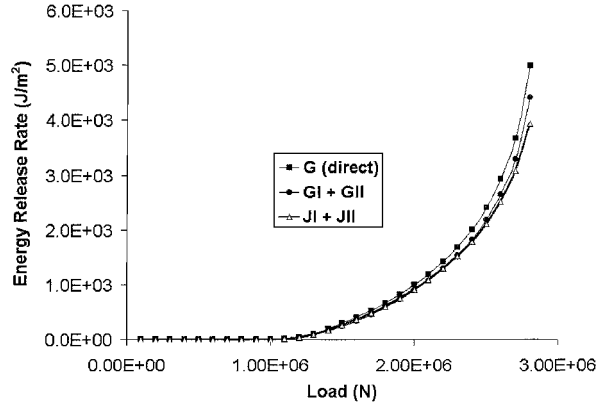

Fig. 24 Displacement-based ($J_{I,\Delta} + J_{II,\Delta}$): bimaterial.

J integral is used to determine mode I and mode II energy release rates.

The new displacement-based method of mode separation has been verified for use in homogeneous and bimaterial cracks. In both cases this new method resulted in an order of magnitude reduction in computational effort as compared to the stress-based method of mode separation. In addition, the method is robust, and one can be quite confident in applying it to homogeneous, as well as bimaterial cracks, something that cannot be said of the stress-based method of mode separation.

Conclusions

The direct method of calculation of the energy release rate has been shown to be robust and reliable. The fact that the method is displacement- not stress-based gives its use credence. For a coarse mesh the total energy release rate may be found accurately with minimal computational effort. Although there exist other methods to compute energy release rates, the direct calculation of the energy release remains the most reliable method for determining the total energy release rate of a laminate.

Accurate (stress-based) mode separation is extremely difficult, even for a crack that exists between similar materials. The results of this method should always be verified against that of the direct calculation of the total energy release rate to certify the mesh refinement used in a finite element analysis. A very finely discretized mesh is necessary to obtain accurate results, and this limits computational efficiency.

For a bimaterial crack, stress-based mode separation has been shown to produce acceptable estimates of the energy release rates. However, the bimaterial stress-based mode separation results were not as accurate as for the homogeneous case, and this was due to the inaccurate modeling of the stresses across the bimaterial interface. Although the stress-based mode separation method may be used for bimaterial cracks, it must be used with caution and only when the method is again verified against the results of a direct calculation of total G.

A new method of mode separation has been developed: It is displacement-based and therefore avoids the difficulties associated with the use of the crack closure integrals. The method does slightly underestimate the total energy release rate, as found by the direct method in the unrestrained case. This underestimation is caused by the restraints imposed, which develop a moment that acts to inhibit crack growth. However, the method is robust, and it certainly is more reliable than the stress-based method of mode separation. Its use resulted in an order-of-magnitude reduction in computational effort as compared to the stress-based method. The method was effective for both homogeneous and bimaterial delaminations.

The J integral is found to be a reliable and effective measure of the total energy release rate for both homogeneous and bimaterial delaminations. A related application of the new method involved the imposition of the appropriate displacement restraints to provide the modal contributions as computed utilizing the J integral (in effect, J_I and J_{II}). This also proved to be a robust and effective method of mode separation, for both homogeneous and bimaterial delaminations. To the best of the authors' knowledge, the J integral has not been employed in this fashion to obtain mode I and mode II energy release rates.

Acknowledgments

The research was supported by the Office of Naval Research under Grant N00014-91-J-1637 of the Ship Structures and Systems S&T Division of the Solid Mechanics Program. The constant interest and encouragement of Yapa D. S. Rajapakse, Program Director, is greatly appreciated.

References

[1]Garg, A. C., "Delamination—A Damage Mode in Composite Structures," *Engineering Fracture Mechanics*, Vol. 29, No. 5, 1988, pp. 557–584.

[2]Wilkins, D. J., Eisenmann, J. R., Camin, R. A., Margolis, W. S., and Benson, R. A., "Characterizing Delamination Growth in Graphite-Epoxy," *Damage in Composite Materials: Basic Mechanisms, Accumulation, Tolerance, and Characterization*, ASTM STP 775, edited by K. L. Reifsnider, American Society for Testing and Materials, Philadelphia, 1982, pp. 168–183.

[3]Rice, J. R., "A Path Independent Integral and the Approximate Analysis of Strain Concentration by Notches and Cracks," *Journal of Applied Mechanics*, Vol. 35, 1968, pp. 379–386.

[4]Rybicki, E. F., and Kanninen, M. F., "A Finite Element Calculation of Stress Intensity Factors by a Modified Crack Closure Integral," *Engineering Fracture Mechanics*, Vol. 9, 1977, pp. 931–938.

[5]Yin, W. L., "The Effects of Laminated Structure on Delamination Buckling and Growth," *Journal of Composite Materials*, Vol. 22, June 1988, pp. 502–517.

[6]Sun, C. T., and Jih, C. J., "On Strain Energy Release Rates for Interfacial Cracks in Bi-Material Media," *Engineering Fracture Mechanics*, Vol. 28, No. 1, 1987, pp. 13–20.

[7]Johnson, M. J., "Delamination Effects in Compressively Loaded Composite Laminates," D.Sc. Dissertation, Dept. of Civil Engineering, Washington Univ., St. Louis, MO, Dec. 1997.

[8]Simitses, G. J., Sallam, S., and Yin, W. L., "Effect of Delamination of Axially Loaded Homogeneous Laminated Plates," *AIAA Journal*, Vol. 23, No. 9, 1985, pp. 1437–1444.

[9]Kardomateas, G. A., and Schmueser, D. W., "Buckling and Postbuckling of Delaminated Composites Under Compressive Loads Including Transverse Shear Effects," *AIAA Journal*, Vol. 26, No. 3, 1988, pp. 337–343.

[10]Anderson, T. L., *Fracture Mechanics, Fundamentals and Applications*, 2nd ed., CRC Press, Boca Raton, FL, 1995, Chap. 11.

[11]Suo, Z., and Hutchinson, J. W., "Interface Crack Between Two Elastic Layers," *International Journal of Fracture*, Vol. 43, 1990, pp. 1–18.

[12]Davidson, B. D., and Krafchak, T. M., "Analysis of Instability-Related Delamination Growth Using a Crack Tip Element," *AIAA Journal*, Vol. 31, No. 11, 1993, pp. 2130–2136.

[13]Davidson, B. D., Hu, H., and Schapery, R. A., "An Analytical Crack-Tip Element for Layered Elastic Structure," *Journal of Applied Mechanics*, Vol. 62, June 1995, pp. 294–305.

[14]Hellen, T. K., "On the Method of Virtual Crack Extensions," *International Journal for Numerical Methods in Engineering*, Vol. 9, 1975, pp. 187–207.

[15]Parks, D. M., "The Virtual Crack Extension Method for Nonlinear Material Behavior," *Computer Methods in Applied Mechanics and Engineering*, Vol. 12, 1977, pp. 353–364.

[16]Parks, D. M., "Virtual Crack Extension: A General Finite Element Technique for J-Integral Evaluation," *Numerical Methods in Fracture Mechanics*, 1977, pp. 464–479.

[17]Beuthe, J. L., and Narayan, S. H., "Separation of Crack Extension Modes in Composite Delamination Problems," *Composite Materials: Fatigue and Fracture*, Vol. 6, ASTM STP 1285, edited by E. A. Armanios, American Society for Testing and Materials, 1997, pp. 324–342.

[18]Davidson, B. D., "Energy Release Rate Determination for Edge Delamination Under Combined In-Plane, Bending and Hygrothermal Loading. Part I—Delamination at a Single Interface," *Journal of Composite Materials*, Vol. 28, No. 11, 1994, pp. 1009–1031.

[19]Davidson, B. D., "Prediction of Energy Release Rate for Edge Delamination Using a Crack Tip Element Approach," *Composite Materials: Fatigue and Fracture*, Vol. 5, ASTM STP 1230, edited by R. H. Martin, American Society for Testing and Materials, 1995, pp. 155–175.

[20]Davidson, B. D., Fariello, P. L., Hudson, R. C., and Sundararaman, V., "Accuracy Assessment of the Singular-Field-Based Mode-Mix Decomposition Procedure for the Prediction of Delamination," *Composite Materials: Testing and Design*, Vol. 13, ASTM STP 1242, edited by S. J. Hooper, American Society for Testing and Materials, 1997, pp. 109–128.

[21]Raju, I. S., "Calculation of Strain-Energy Release Rates with Higher Order and Singular Finite Elements," *Engineering Fracture Mechanics*, Vol. 28, No. 3, 1987, pp. 251–274.

[22]Raju, I. S., Crews, J. H., and Aminpour, M. A., "Convergence of Strain Energy Release Rate Components for Edge-Delaminated Composite Laminates," *Engineering Fracture Mechanics*, Vol. 30, No. 3, 1988, pp. 383–396.

[23]Beuthe, J. L., "Separation of Crack Extension Modes in Orthotropic Delamination Models," *International Journal of Fracture*, Vol. 77, 1996, pp. 305–321.

[24]Hashemi, S., Kinloch, A. J., and Williams, G., "Mixed-Mode Fracture in Fiber-Polymer Composite Laminates," *Composite Materials: Fatigue and Fracture*, Vol. 3, ASTM STP 1110, edited by T. K. O'Brien, American Society for Testing and Materials, Philadelphia, 1991, pp. 143–168.

[25]Kinloch, A. J., Wang, Y., Williams, J. G., and Yayla, P., "The Mixed-Mode Delamination of Fiber Composite Materials," *Composites Science and Technology*, Vol. 47, 1993, pp. 225–237.

[26]Charalambides, M., Kinloch, A. J., Wang, Y., and Williams, J. G., "On the Analysis of Mixed-Mode Failure," *International Journal of Fracture*, Vol. 54, 1992, pp. 269–291.

A. M. Waas
Associate Editor